

# Removal of uranium(VI) from aqueous solution using citric acid modified pine sawdust: batch and column studies

Weihua Zou · Lei Zhao

Received: 10 September 2011 / Published online: 4 October 2011  
© Akadémiai Kiadó, Budapest, Hungary 2011

**Abstract** This study described adsorption of uranium(VI) by citric acid modified pine sawdust (CAMPS) in batch and fixed-bed column modes at 295 K. The equilibrium adsorption data were analyzed by Langmuir, Freundlich, Koble–Corrigan and Dubinin–Radushkevich isotherm models. The results indicated that the Langmuir and Koble–Corrigan models provided the best correlation of the experimental data. The Elovich model was better to fit the kinetic process, which suggested that ion exchange was one of main mechanism. The effective diffusion parameter  $D_t$  values indicated that the intraparticle diffusion was not the rate-controlling step. In fixed-bed column adsorption, the effects of bed height, feed flow rate, and inlet uranium (VI) concentration were studied by assessing breakthrough curve. The Thomas, the Yan and the bed-depth/service time (BDST) models were applied to the column experimental data to determine the characteristic parameters of the column adsorption. The results were implied that CAMPS may be suitable as an adsorbent material for adsorption of uranium (VI) from an aqueous solution.

**Keywords** Uranium(VI) · Citric acid modified pine sawdust · Adsorption · Isotherm · Fixed-bed column

## Introduction

Uranium, a toxic and weak radioactive heavy metal, is relatively widespread in the environment, and as a

naturally occurring element it is found at low levels in all rocks, soils and waters [1]. But uranium mining, milling, processing, enriching, and disposal all contribute to contaminate surface water and groundwater, where the concentrations of uranium may increase to above  $1 \mu\text{g L}^{-1}$ . In the aquatic environment, uranium usually occurs in the hexavalent form as a mobile, hydrated uranyl  $\text{UO}_2^{2+}$  ion. Its solubility is strongly dependent on the pH of its solution. Uranium(VI) is extremely mobile and once entered the living bodies provoke the inner irradiation (especially due to the g-active decay products), having as a final result the appearance of cancer [2]. To overcome these disadvantages of the release of uranium to the environment, some waste water treatment techniques must be used. Several techniques are available for the removal of U(VI) ions from aqueous solutions including chemical precipitation, ion-exchange, membrane processes, solvent extraction and adsorption being the most commonly used methods employed [3–10]. Of these various methods, adsorption has proved to be an effective and attractive process [6]. Activated carbon is commonly used as an adsorbent for removing uranium(VI) from wastewater due to its excellent adsorption capabilities [9]. However, its high cost limits its widespread use. Therefore, interest is growing to find alternatives to carbon adsorbents. Recently, attention has been focused on the development of low-cost adsorbents for applications concerning treatment of wastewater [1, 11–14]. Adsorption by low cost adsorbents provides an environmentally and economically favorable method for removing uranium from wastewaters [11].

Agricultural by-products, such as, rice straw, wood powder and wheat straw, have been studied for uranium(VI) removal from wastewater [1, 12–14]. Generally, the sorption capacities of crude agricultural by-products are low. For improving the sorption capacity of crude agricultural

W. Zou (✉) · L. Zhao  
School of Chemical Engineering and Energy,  
Zhengzhou University, 100# of Kexue Road,  
Zhengzhou 450001, People's Republic of China  
e-mail: whzou@zzu.edu.cn

by-products, chemical modification was used [15, 16]. Modification of agricultural by-products can be carried out to achieve adequate structural durability, enhance their natural ion exchange capability and add value to the by-product [15, 17]. Sawdust is a waste by-product of the timber industry that is either used as cooking fuel or a packing material. Wood powder does not noticeably swell in water and does not decompose upon prolonged contact with water. It can be used as a low-cost adsorbent largely due to its lignocellulosic composition. It contains abundant lignin, cellulose, hemicellulose and some functional groups such as carboxyl, hydroxyl, phenolic and amide groups, etc. in its structure, which make the adsorption processes possible [18]. A number of publications have reported on the use of wood sawdust to remove contamination from solution [18, 19]. But modified pine sawdust with citric acid (CAMPS) as adsorbent for removal of uranium(VI) from solution is not studied.

In this study, CAMPS was used to remove uranium(VI) ions from aqueous solution in batch and fixed bed column systems. The objectives were to: (i) perform batch studies to examine uranium(VI) adsorption using CAMPS (effect of initial uranium concentration and pH, adsorption isotherm and kinetics) and (ii) perform column studies to investigate the uranium(VI) uptake characteristics of CAMPS under different flow rates, different bed height and different initial uranium(VI) concentration.

## Experimental

### Materials

#### Preparation of CAMPS

Natural pine sawdust (NPS) used obtained from a local sawmill in Zhengzhou City, R.P. China. It was washed several times with distilled water to remove surface impurities, and this was followed by drying for 8 h at 60 °C in the oven. The dry pine sawdust was crushed into powder and sieved to 20–40 mesh fractions for chemical modification.

Citric acid modified pine sawdust (CAMPS) was prepared according to the modified method [15]. Ground pine sawdust was mixed with 0.6 mol L<sup>-1</sup> citric acid at the ratio of 1:12 (pine sawdust/acid, w/v) and stirred for 30 min at 20 °C. The acid pine sawdust slurries were placed in a stainless steel tray and dried at 50 °C in a forced air oven for 24 h. Then the thermo-chemical esterification between acid and pine sawdust was proceeded by raising the oven temperature to 120 °C for 90 min. After cooling, the esterified pine sawdust was washed with distilled water

until the liquid did not turn turbidity when 0.1 mol L<sup>-1</sup> CaCl<sub>2</sub> was dropped in. After filtration, CAMPS was suspended in 0.1 mol L<sup>-1</sup> NaOH solution at suitable ratio and stirred for 60 min, followed by washing thoroughly with distilled water to remove residual alkali, next dried at 50 °C for 24 h and preserved in a desiccator for use.

### Reagents

All chemicals and reagents used for experiments and analyses were of A.R. grade. The solution of uranium(VI) was prepared by dissolving accurately weighted amount of UO<sub>2</sub>(NO<sub>3</sub>)<sub>2</sub>·6H<sub>2</sub>O (A.R.) in deionized water. The initial pH values of the working solutions were adjusted by the addition of HNO<sub>3</sub> or NaOH solutions. Arsenazo III solution was prepared by dissolving 0.5 g of the reagent in 1000 mL of de-ionized water. Fresh dilutions were employed for each experiment.

### Determination of the U(VI) ion content of the solutions

A simple and sensitive spectrophotometric method based on coloured complexes with arsenazo III in an aqueous medium was used for the determination of the uranium(VI) ion concentration [20]. The concentration of uranium(VI) ions in solution was determined spectrophotometrically by absorbance measurements at  $\lambda_{\text{max}} = 588 \text{ nm}$  using a Shimadzu Brand UV-3000 spectrophotometer.

### Equilibrium studies

The batch adsorption was performed using water bath shakers at 295 K and at a constant agitation speed of 120 rpm. In this study 20 mL of uranium(VI) solution was agitated with 3.0 g L<sup>-1</sup> of CAMPS in 50 mL flask. Contact time was carried out at initial dye concentrations of 120 mg L<sup>-1</sup>.

Equilibrium experiments were performed with different initial uranium(VI) concentration. The agitated time was 180 min to reach equilibrium. The effect of pH on adsorption of uranium(VI) onto CAMPS was investigated by varying the initial solution pH from 2.0 to 10.0.

The amount of dye adsorbed onto the unit weight of the adsorbent ( $q_t$  or  $q_e$ , mg g<sup>-1</sup>) was calculated using the following equations:

$$q_e = \frac{V(C_0 - C)}{m} \quad (1)$$

where  $V$  is the solution volume in L;  $C_0$  is the initial concentration in mg L<sup>-1</sup>,  $C$  is the uranium(VI) concentration at any time in mg L<sup>-1</sup>, and  $m$  is the weight of adsorbent in g.

## Column studies

Continuous adsorption experiments in a fixed-bed column were conducted in a glass column (1.0 cm ID and 30 cm height), packed with a known quantity of CAMPS. A known concentration of uranium(VI) solution was pumped in down flow mode at desired flow rates using a peristaltic pump. Samples were collected at regular intervals. The effects of the following column parameters, on uranium(VI) adsorption were investigated. (i) Effect of bed height: bed height was varied between 7.0 cm (1.42 g), 10.0 cm (2.10 g) and 13.0 cm (2.66 g), keeping flow rate and initial uranium(VI) concentration constant at 8 mL min<sup>-1</sup> and 60 mg L<sup>-1</sup>, respectively. (ii) Effect of flow rate: flow rate was varied between 6 and 10 mL min<sup>-1</sup>, while bed height and inlet uranium(VI) concentration were held constant at 10.0 cm and 60 mg L<sup>-1</sup>, respectively. (iii) Effect of initial uranium(VI) concentration: inlet uranium(VI) concentration was varied between 40, 80 mg L<sup>-1</sup>, at 10.0 cm bed height and 8 mL min<sup>-1</sup> flow rate.

The loading behaviour of U(VI) ions adsorbed from aqueous solution onto a fixed bed is usually expressed in term of  $C/C_0$  ( $C$  = effluent metal ion concentration;  $C_0$  = influent metal ion concentration) as a function of time or the volume of the effluent for a given bed height, thereby allowing the corresponding breakthrough curve to be constructed [21]. The maximum column capacity,  $q_{total}$  (mg), for a given feed concentration and flow rate,  $Q$ , is equal to the area under the curve of adsorbed U(VI) ion concentration,  $C_{ads}$  ( $C_{ads} = C_0 - C$ ) (mg L<sup>-1</sup>), versus time (min) and is calculated via Eq. 1:

$$q_{total} = \frac{QA}{1000} = \frac{Q}{1000} \int_{t=0}^{t=t_{total}} C_{ad} dt \quad (2)$$

The equilibrium uptake ( $q_e'$ ), the amount of uranium(VI) ions adsorbed per unit mass of dry adsorbent (mg g<sup>-1</sup>) in the column, is calculated from:

$$q_e' = q_{total}/X \quad (3)$$

where  $X$  is the total mass of dry adsorbent in the column.

## Results and discussion

### Batch studies

#### Effect of pH

The  $pH_{zpc}$  of an adsorbent is a very important characteristic that determines the pH at which the adsorbent surface has net electrical neutrality. The determination of  $pH_{zpc}$  of CAMPS was performed according to the solid addition method [22]: 20 mL of 0.01 mol L<sup>-1</sup> KNO<sub>3</sub> solution was

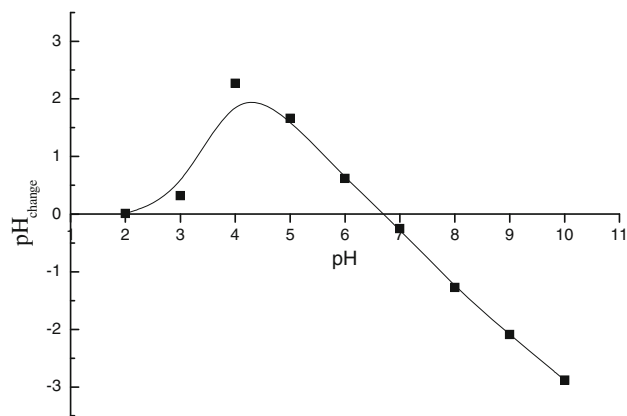


**Fig. 1** The zero point of charge ( $pH_{zpc}$ ) of CAMPS

placed in conical flasks. The initial pH of the solutions was adjusted to a value between 2 and 11 by adding 0.1 mol L<sup>-1</sup> HCl or NaOH solution. Then 0.1 g of CAMPS was added to each flask, stirred and the final pH of the solutions was measured after 24 h. The value of  $pH_{zpc}$  can be determined from the curve that cuts the  $pH_i$  line of the plot  $\Delta pH$  versus  $pH_i$  (Fig. 1).

The pH of solution could affect the solubility and speciation of metal ions in solution. The influence of solution pH on adsorption process can also be interpreted with the help of the structure and surface charge of the adsorbent. The relative abundance of various uranium(VI) species is a strong function of pH and composition of solution. In the absence of carbonates, complexation of uranium(VI) and hydroxyl ion is a possible reaction, while in the presence of carbonates, the reaction of uranyl ion with  $CO_3^{2-}$  is the most dominant reaction in aqueous medium.

The no precipitate of U(VI) and colloid formation were observed in the pH range of 2.0–10.0 under the experimental condition. The experimental results are shown in Fig. 2. As shown in Fig. 2, the pH of aqueous phase is a controlling factor in uranium(VI) adsorption. Under higher acidic conditions, uranium(VI) uptake was minimal. This may be explained by considering the zero point of charge ( $pH_{zpc}$ ) for the CAMPS. The zero point of charge is a concept in physical chemistry relating to the phenomenon of adsorption, and it describes the condition when the electrical charge density on a surface is zero. The plot of change in solution pH ( $\Delta pH$ ) versus initial pH ( $pH_i$ ) showed that with increasing initial solution pH, the pH change become more negative and the zero value of  $\Delta pH$  was reached at  $pH_i$  value of 6.7, which is considered as the  $pH_{zpc}$  of CAMPS. If the pH was below  $pH_{zpc}$  of CAMPS, more of the surface sites were positive charged and uranium(VI) will be adsorbed to a lesser extent due to the repulsive forces between uranium(VI) ions and positive charge of the CAMPS surface. So, as pH increased from

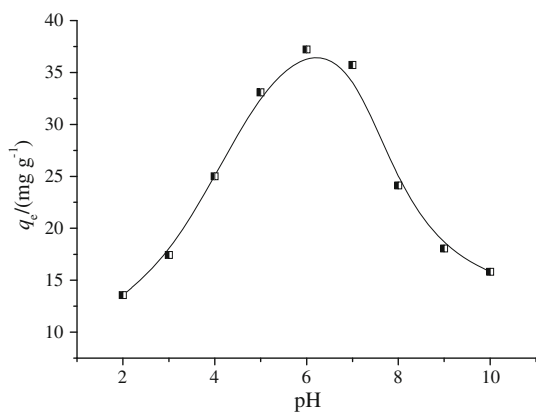


**Fig. 2** Effect of initial pH on adsorption of uranium (VI) by CAMPS (CAMPS dose  $3 \text{ g L}^{-1}$ ,  $C_0$ :  $150 \text{ mg L}^{-1}$ )

2.0 to 6.5, the fraction of uranium(VI) adsorbed on CAMPS increased. Adsorption reached a maximum at pH of 6.5. However, if the pH was above  $\text{pH}_{\text{zpc}}$ , the surface charge is negatively, more uranium(VI) ions should be adsorbed, but the result showed that the extent of adsorption diminished as pH continued to rise from 6.5 to 10.0. This behavior may be explained by that the carbonate concentration increases with pH at a constant carbon dioxide partial pressure, resulting in an increase in the concentration of soluble uranium(VI) carbonate complexes. The behavior of uranium(VI) ions in aqueous solution is a complex phenomenon in the sense that uranium(VI) ions may be present as ions of different composition. Uranium(VI) basically exists as free uranyl ion, its hydrolysis complexes, and multinuclear hydroxide and carbonate complexes as a function of pH and uranium(VI) concentration under experimental conditions. At pH 7.0–10.0, the solution carbonate complexes of  $\text{UO}_2^{2+}$  such as  $\text{UO}_2(\text{CO}_3)_2^{2-}$  and  $\text{UO}_2(\text{CO}_3)_3^{4-}$ , are the dominant anion species. They compete with uranium(VI) ions for adsorption sites, so that the adsorption of uranium(VI) ions decreases as the concentration of dissolved carbonate and bicarbonate anions increase [23]. Therefore, all the adsorption experiments were carried out at pH 6.5.

#### Equilibrium study

The effect of  $C_e$  on adsorption is shown in Fig. 3. The values of  $q_e$  increased with increasing  $C_e$ . The uranium(VI) concentration provided the necessary driving force to overcome the resistances to the mass transfer of uranium(VI) between the aqueous and solid phases. The increase in  $C_e$  also enhanced the interaction between uranium(VI) and CAMPS. Therefore, an increase in  $C_e$  of uranium(VI) enhanced the adsorption uptake of uranium(VI).

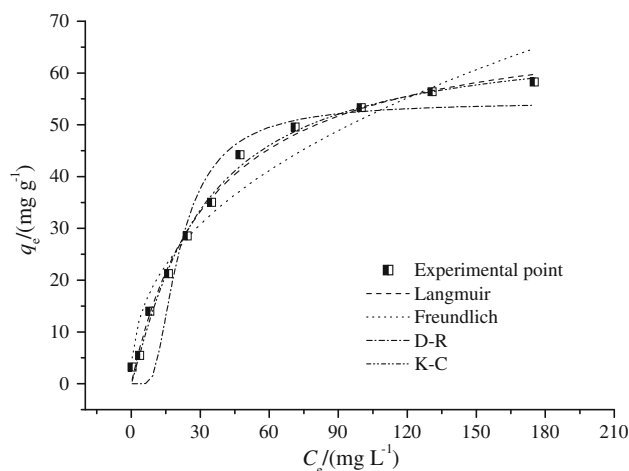


**Fig. 3** Experimental points and fitted isotherm curves

In this article, the Langmuir, Freundlich, Koble–Corrigan and Dubinin–Radushkevich isotherm models were used to describe the adsorption equilibrium.

The Langmuir adsorption isotherm has been successfully applied to many pollutants adsorption processes and has been the most widely used sorption isotherm for the sorption of a solute from a liquid solution [24]. The common form of the Langmuir isotherm is:

$$q_e = \frac{q_m K_L c_e}{1 + K_L c_e} \quad (4)$$

where  $q_m$  is the  $q_e$  for a complete monolayer ( $\text{mg g}^{-1}$ ), a constant related to adsorption capacity; and  $K_L$  is a constant related to the affinity of the binding sites and energy of adsorption ( $\text{L mg}^{-1}$ ).

The Freundlich isotherm is an empirical equation describing adsorption onto a heterogeneous surface. The Freundlich isotherm is commonly presented as [25]:

$$q_e = K_F c_e^{1/n} \quad (5)$$

where  $K_F$  and  $1/n$  are the Freundlich constants related to the adsorption capacity and adsorption intensity of the adsorbent, respectively.

The Koble–Corrigan model is a three-parameters equation for the representing equilibrium adsorption data. It is a combination of the Langmuir and Freundlich isotherm type models and is given by Eq. 6 [26]:

$$q_e = \frac{A C_e^n}{1 + B C_e^n} \quad (6)$$

where  $A$ ,  $B$  and  $n$  are the Koble–Corrigan parameters.

The Dubinin–Radushkevich (D–R) model, which does not assume a homogeneous surface or a constant adsorption potential as the Langmuir model, was further used to test the experimental data [27]. The D–R isotherm is given as Eq. 7

**Table 1** Isotherm constants for uranium (VI) adsorption onto CAMPS

Isotherm	Parameters	Value	$R^2$	SS
Langmuir	$q_m$ (mg g <sup>-1</sup> )	71.59 ± 2.10	0.9941	0.734
	$K_L$ (L mg <sup>-1</sup> )	0.029 ± 0.002		
Freundlich	$K_F$	7.311 ± 1.479	0.9512	8.556
	$1/n_F$	0.422 ± 0.045		
Dubinin–Radushkevich	$q_m$ (mg g <sup>-1</sup> )	54.36 ± 3.071	0.9197	16.592
	$k$ (mmol <sup>2</sup> J <sup>-2</sup> ) × 10 <sup>-10</sup>	8.827 ± 1.879		
	$E$ (kJ mol <sup>-1</sup> )	23.80		
Koble–Corrigan	$A$	1.426 ± 0.417	0.9952	0.489
	$B$	0.021 ± 0.005		
	$n$	1.132 ± 0.102		

<sup>a</sup>  $SS = \sum \frac{(q_{e,exp} - q_{e,cal})^2}{q_{e,cal}}$ ,  $q_{e(exp)}$  and  $q_{e(cal)}$  are the experimental value and calculated value according the model, respectively

$$q_e = q_m \exp(-k\varepsilon^2) \quad (7)$$

where,  $\varepsilon$  ( $RT \ln(1 + 1/C_e)$ ) is the Polanyi potential,  $q_m$  (mg g<sup>-1</sup>) is the adsorption capacity, and  $k$  (mol<sup>2</sup> kJ<sup>-2</sup>) is a constant related to the adsorption energy when it is transferred to the surface of the solid from infinity in the solution. This energy ( $E$ ) can be computed using the following relationship (Eq. 8) [28]:

$$E = \frac{1}{\sqrt{2k}} \quad (8)$$

All relative parameters of the isotherm equations, the values of  $R^2$  and  $SS$  are listed in Table 1, respectively. Figure 3 depicts the experimental equilibrium data and the fitted equilibrium curves by four various isotherms, respectively.

It was obvious that regression coefficients ( $R^2$ ) obtained from the Koble–Corrigan and Langmuir isotherms were higher than that of the Freundlich and Dubinin–Radushkevich isotherms while the relative values of  $SS$  were lower, respectively, which suggested the applicability of the Koble–Corrigan and Langmuir isotherms for uranium(VI) adsorption onto CAMPS.

According to Langmuir constants, the maximum monolayer adsorption capacity ( $q_m$ ) of CAMPS for uranium(VI) was 71.6 mg g<sup>-1</sup>. The reported values of  $q_m$  about some materials in literatures are 40.5 mg g<sup>-1</sup> for coffee residues [29], 71.4 mg g<sup>-1</sup> for olive cake, 99.96 mg g<sup>-1</sup> for wood powder and 47.6 mg g<sup>-1</sup> for wheat straw [14], respectively. As a low cost adsorbent, CAMPS exhibits the potential for the removal of uranium(VI) from aqueous solution. The carboxyl groups on the surface of the modified pine sawdust (CAMPS) were primarily responsible for the sorption of uranium(VI).

In this study, the  $E$  value calculated from Eq. 10 was calculated as 23.80 kJ mol<sup>-1</sup> for uranium(VI) on CAMPS. The parameter gives information about the type of adsorption mechanism as chemical ion-exchange or physical adsorption. If the magnitude of  $E$  is between 8 and 16 kJ mol<sup>-1</sup>, the sorption process is supposed to proceed via chemisorption, while for values of  $E < 8$  kJ mol<sup>-1</sup>, the sorption process is of physical nature [30]. This result indicates that the adsorption mechanism was chemical ion-exchange.

### Kinetic study

The effect of contact time on uranium(VI) adsorption was shown in Fig. 4. From Fig. 4, a two-stage kinetic behavior was evident. A very rapid initial adsorption over 40 min, followed by a longer period of considerably slower uptake. With the beginning of adsorption, the values of  $q_t$  increased quickly and then the change turned slow after 40 min. After 180 min, the adsorbed quantity of uranium(VI) showed nearly no change.

In this study, the pseudo-first order kinetic model, pseudo-second order kinetic model, Elovich and intra-particle diffusion model were used to analyze the adsorption kinetics for the adsorption of uranium(VI).

The pseudo-first order kinetic model is expressed as [31]:

$$q_t = q_e(1 - e^{-k_1t}) \quad (9)$$

The pseudo-second order kinetic model is given by the following equation as [31]:

$$q_t = \frac{k_2q_e^2t}{1 + k_2q_e t} \quad (10)$$

where  $q_e$  and  $q_t$  are the amount of uranium(VI) adsorbed per unit weight of the adsorbent at equilibrium and at any

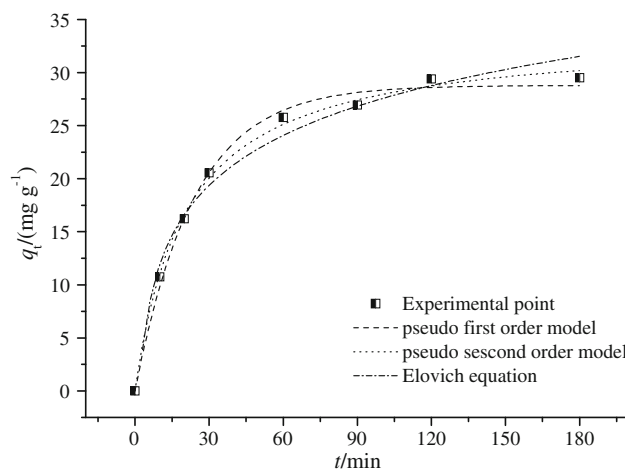


**Fig. 4** Effect of contact time on the adsorption and fitted curves ( $C_0$ : 100 mg L<sup>-1</sup>.)



time  $t$ , respectively ( $\text{mg g}^{-1}$ ) and  $k_1$  is the rate constant of pseudo-first order adsorption ( $\text{min}^{-1}$ );  $k_2$  is the rate constant of pseudo-second order adsorption ( $\text{g mg}^{-1} \text{min}^{-1}$ ).

The Elovich model is expressed as [32]:

$$q_t = A_E + B_E \ln t \quad (11)$$

where  $A_E$  and  $B_E$  are the Elovich constant.

The intraparticle diffusion model [33]:

$$q_t = Kt^{1/2} + C \quad (12)$$

$K$  is the intraparticle diffusion rate constant ( $\text{g mg}^{-1} \text{min}^{-1/2}$ ),  $C$  is a constant that gives idea about the thickness of the boundary layer, i.e., larger the value of  $C$  the greater is the boundary layer effect.

The kinetic constants can be determined using nonlinear regressive analysis according to experimental data. The parameters are listed in Table 2. The fitted curves are also shown in Fig. 4.

From Table 2, the values of  $R^2$  were bigger than 0.986 and values of  $SS$  were less than 0.501. So it was reasonable for all the three models to be used to predict the effect of contact time on adsorption.

As the Elovich equation is successfully used to describe the adsorption kinetics of ion exchange systems, it can be concluded that the adsorption system be a chemical process, especially an ion exchange process [32]. There was negative charge of carboxyl group ( $-\text{COO}^-$ ) on the surface of CAMPS, but uranium(VI) existed in solution were positive. So it was referred that the main mechanism of uranium(VI) adsorption behavior by CAMPS may be ion exchange. This result is also consistent with the foregoing

conclusion derived from the mean free energy of adsorption ( $E$ ) in the D-R isotherm.

From intraparticle diffusion model,  $K_t$  is the intraparticle diffusion rate constant ( $\text{g mg}^{-1} \text{min}^{-1/2}$ ),  $C$  is a constant that gives idea about the thickness of the boundary layer. The result of regression analysis of the data is also presented in Table 2, from which it is seen that the regression estimates of the first linear segment indicated an intercept value differing from zero, thereby suggesting that pore diffusion was not the sole step controlling the overall rate of mass transfer at the start of batch adsorption. Film-diffusion control may also have occurred during these early stages of the adsorption process and may have still been controlling the rate of mass transfer during the time period of the first linear segment [34]. This shows that the mechanism of uranium(VI) adsorption onto CAMPS is complex and both the surface adsorption and intra-particle diffusion contribute to the actual adsorption process.

The half-adsorption time  $t_{1/2}$  was another parameter which can be calculated from the equilibrium concentration and the diffusion coefficient rate values. This was calculated by using the following equation [35]:

$$t_{1/2} = \frac{1}{k_2 q_e} \quad (13)$$

where  $k_2$  and  $q_e$  can be obtained from Table 3.

The diffusion coefficient for the intraparticle transport of uranium(VI) was also calculated by using the following relationship [35]:

$$t_{1/2} = \frac{0.03r^2}{D_i} \quad (14)$$

**Table 2** Kinetic constants for uranium(VI) adsorption onto CAMPS

Kinetic model	Parameters	Value	Parameters	Value	$R^2$	$SS$
Pseudo first order	$k_1$ ( $\text{min}^{-1}$ )	0.0418	$q_{1(\text{cal})}$ ( $\text{mg g}^{-1}$ )	28.79	0.9949	0.194
Pseudo second order	$k_2$ ( $\text{g mg}^{-1} \text{min}^{-1}$ )	$1.47 \times 10^{-3}$	$q_{2(\text{cal})}$ ( $\text{mg g}^{-1}$ )	33.59	0.9972	0.039
Elovich	$A_E$	-3.38	$B_E$	6.78	0.9865	0.501
Intraparticle diffusion (1)	$k_{t1}$ ( $\text{mg g}^{-1} \text{min}^{-1/2}$ )	3.42	$C_1$ ( $\text{mg g}^{-1}$ )	0.375	0.9950	0.375
Intraparticle diffusion (2)	$k_{t2}$ ( $\text{mg g}^{-1} \text{min}^{-1/2}$ )	0.707	$C_1$ ( $\text{mg g}^{-1}$ )	20.55	0.9152	0.059

**Table 3** Thomas parameters at different conditions

$C_0$ ( $\text{mg L}^{-1}$ )	$Q$ ( $\text{mL min}^{-1}$ )	$Z$ (cm)	$q_{\text{total}}$ (mg)	$q_e'$ ( $\text{mg g}^{-1}$ )	$k_{\text{Th}}$ ( $\text{mL mg}^{-1} \text{min}^{-1}$ )	$q_0$ ( $\text{mg g}^{-1}$ )	$R^2$
60	8.0	7	64.80	45.63	0.338	40.84	0.9831
60	8.0	10	100.49	47.85	0.281	57.38	0.9856
60	8.0	13	129.38	48.64	0.208	73.97	0.9728
40	8.0	10	92.8	44.19	0.345	52.63	0.9853
80	8.0	10	108.8	51.81	0.208	62.02	0.9818
60	6.0	10	111.6	53.14	0.201	81.31	0.9875
60	10.0	10	90.00	42.86	0.331	45.06	0.9871

$$D_i = \frac{0.03r^2}{t_{1/2}} = 0.03k_2q_e r^2 \quad (15)$$

where  $t_{1/2}$  is the half life in seconds as calculated from Eq. 13,  $r$  is the radius of the adsorbent particle in centimeters and  $D_i$  is the diffusion coefficient value in  $\text{cm}^2 \text{s}^{-1}$ . According to Singh et al. [36], a value of  $D_i$  of the order of  $10^{-10}$ – $10^{-11} \text{ cm}^2 \text{ s}^{-1}$  indicates that intra-particle diffusion is rate-limiting step in the adsorption process. In this study, the value of  $D_i$  was  $5.57 \times 10^{-6} \text{ cm}^2 \text{ s}^{-1}$ , which is three orders of magnitude greater than the value quoted by Singh et al. [36]. This indicates that intraparticle diffusion is not the rate-controlling step.

## Column studies

### Effect of flow rate on breakthrough curve

The breakthrough curves at various flow rates are shown in Fig. 5 where it can be seen that the breakthrough generally occurred faster with a higher flow rate. Breakthrough time reaching saturation was increased significantly with a decrease in the flow rate. At a low rate of influent, uranium(VI) had more time to be in contact with adsorbent, which resulted in a greater removal of uranium(VI) ions in column. Hence lower flow rates were desirable for the effective removal of uranium(VI) in column mode.

### Effect of influent uranium(VI) concentration on breakthrough curve

The breakthrough time decreased with increasing influent uranium(VI) concentration (Fig. 6). As the inlet uranium(VI) concentration increased, much sharper

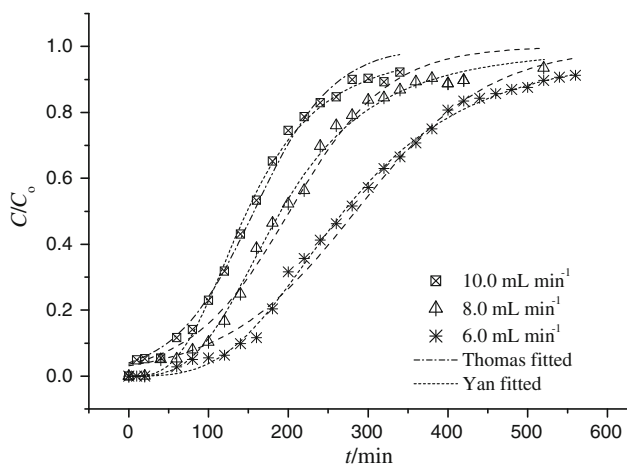


**Fig. 5** Comparison of the experimental and predicted breakthrough curves obtained at different flow rate according to the Thomas and Yan model

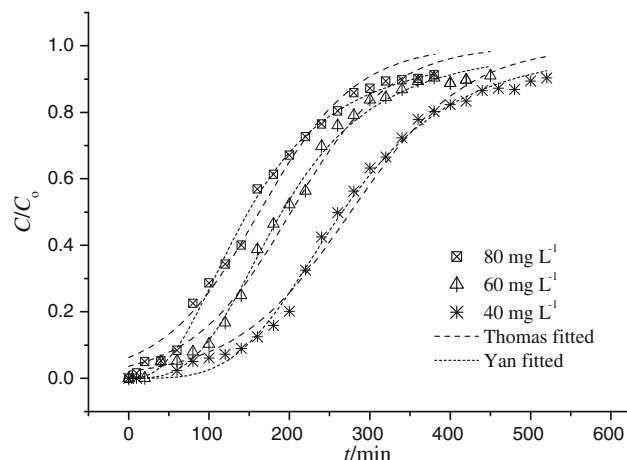


**Fig. 6** Comparison of the experimental and predicted breakthrough curves obtained at different concentration of uranium(VI) according to the Thomas and Yan model

breakthrough curves were observed. As influent uranium(VI) concentration increased, sharper breakthrough curves were obtained [37]. The lowest uranium(VI) concentration resulted in a delayed breakthrough curve since the lower concentration gradient causes reduced transport of uranium(VI). The driving force for adsorption is the concentration difference between the solute on the adsorbent and the solute in the solution [37]. High concentration differences provide a higher driving force, which favors the adsorption process. At high initial dye concentrations, a sharper breakthrough curve indicated shortened mass transfer zone and higher adsorption rates [38]. Therefore, when quick uranium(VI) uptake is desired, which is often the case, operating with high initial uranium(VI) concentrations appears to be favorable [38]. The change of concentration gradient affected the saturation rate and breakthrough time [37].

### The effect of different bed depth on the breakthrough curve

The breakthrough curves at different bed depths were also shown in Fig. 7, respectively. From Fig. 7, it was seen that as the bed height increased, uranium(VI) had more time to contact with CAMPS that resulted in higher removal efficiency of uranium(VI). So the higher bed column resulted in a decrease in the solute concentration in the effluent at the same time. The slope of breakthrough curve decreased with increasing bed height, which resulted in a broadened mass transfer zone. Higher uptake was observed at the highest bed height due to an increase in the surface area of the adsorbent, which provided more binding sites for the sorption [39].

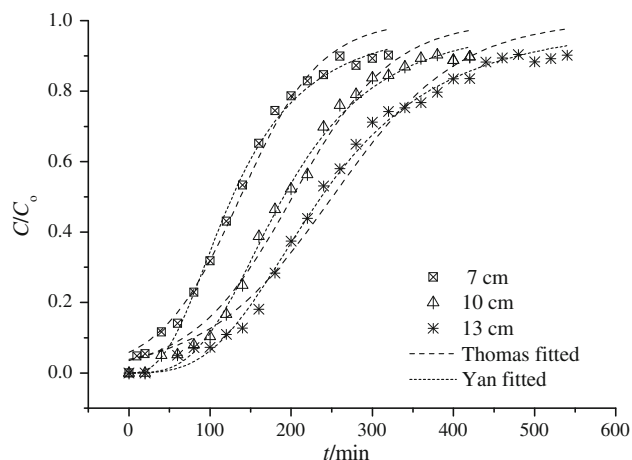


**Fig. 7** Comparison of the experimental and predicted breakthrough curves obtained at different bed depth according to the Thomas and Yan model

### Estimation of breakthrough curves

**Thomas model** The Thomas model, based on the Langmuir adsorption–desorption kinetics, is one of the most widely used models [40]. It assumes no axial dispersion and adsorption is the rate driving force and obeys second-order reversible reaction kinetics [40]. Thomas’ solution also assumes a constant separation factor but it is applicable to either favorable or unfavorable isotherms. The non-linear form of the model may be expressed as in Eq. 16:

$$\frac{C}{C_0} = \frac{1}{1 + \exp(k_{Th}q_0X/Q - k_{Th}C_0t)} \quad (16)$$

where  $k_{Th}$  is the Thomas rate constant ( $\text{mL min}^{-1}\text{mg}^{-1}$ ),  $q_0$  is the uptake of uranium(VI) per g of adsorbent at equilibrium ( $\text{mg g}^{-1}$ ),  $X$  is the mass of adsorbent in the column (g);  $C_0$  is the influent uranium(VI) ion concentration ( $\text{mg L}^{-1}$ ),  $C$  is the effluent concentration at time  $t$  ( $\text{mg L}^{-1}$ ) and  $Q$  is the flow rate ( $\text{mL min}^{-1}$ ). The value of  $C/C_0$  is the ratio of the effluent and influent uranium(VI) ion concentrations, while the time,  $t$ , is expressed in min.

From Table 3, it is seen that the values of the correlation coefficients ( $R^2$ ) ranged from 0.973 to 0.988. Hence, the correlation between  $C/C_0$  and time as expressed in Eq. 16 was significant. The values of  $k_{Th}$  became bigger with the flow rate increasing while the values of  $q_0$  became bigger with initial dye concentration increasing. With the bed depth increasing, the values of  $k_{Th}$  became smaller while the value of  $q_0$  increased. Adsorption capacity depended mainly upon the amount of the adsorbent available for adsorption. The breakthrough time and exhaustion time increased with the increase in bed height since more time was required to exhaust more adsorbent. But the slope of the breakthrough curve decreased as the bed height

increased. This was due to an increase in the axial dispersion of the dye over the column with an increase in column height. This increase in bed height resulted in an increase in the volume of the dye solution treated and therefore a higher percentage of uranium(VI) removal.

Figures 5, 6 and 7 also show a comparison between the breakthrough curves obtained experimentally (full lines) and those predicted using the Thomas model (dotted lines) under various conditions. It is clear from all the figures that the curves predicted at normalized concentrations were in very good agreement with the experimental values. The Thomas model is suitable for adsorption processes where external and internal diffusion are not the rate-limiting steps [37].

### The Yan model

The Yan model [41] is also used to describe the column adsorption data. Use of this model can minimize the error resulting from the use of the Thomas model, especially at lower or higher time periods of the breakthrough curve.

The expression is given as:

$$\frac{C_t}{C_0} = 1 - \frac{1}{1 + \left(\frac{vt}{b}\right)^a} \quad (17)$$

where  $a$  and  $b$  are the constants of the Yan model, respectively. From value of  $b$ , the value of  $q_0$  can be estimated using following equation [41]:

$$q_0 = \frac{bC_0}{X} \quad (18)$$

The model constants ( $a$  and  $b$ ) and values of  $q_0$  are given in Table 4 using nonlinear regressive analysis. From Table 4, they were all fitted with higher determined coefficients ( $R^2$ ) ranging from 0.992 to 0.998. The values of  $q_0$  in Table 4 are smaller than those in Table 3. The breakthrough curves predicted by the Thomas model and the Yan model are also shown in Figs. 5, 6 and 7. At all conditions examined, the predicted breakthrough curves from the Yan model showed reasonably better agreement with the experimental curves than the Thomas model. At the lower and high time of breakthrough curves, the fitted curves of the Thomas model were far from experimental points. So the Yan model was better to predict the uranium(VI) column adsorption than the Thomas model. The trend of values of  $q_0$  and  $b$  in Table 4 is similar to values of  $q_0$  in Table 3 with the change of experimental conditions. Several researchers studied the metal removal by adsorption in the column mode, and found that that the column kinetics could be described more adequately by the Yan model than by the Thomas model [41–43]. Our study on uranium(VI) removal in column adsorption had similar results.



**Table 4** Yan parameters at different conditions

$C_0$ (mg L <sup>-1</sup> )	$Q$ (mL min <sup>-1</sup> )	$Z$ (cm)	$a$	$b$ (mL)	$q_0$ (mg g <sup>-1</sup> )	$R^2$
60	8.0	7	2.650	1019	43.06	0.9922
60	8.0	10	3.252	1523	43.51	0.9956
60	8.0	13	3.038	1903	42.92	0.9955
40	8.0	10	3.719	2125	40.48	0.9962
80	8.0	10	2.518	1190	45.33	0.9950
60	6.0	10	3.267	1618	46.23	0.9976
60	10.0	10	3.034	1486	42.46	0.9947

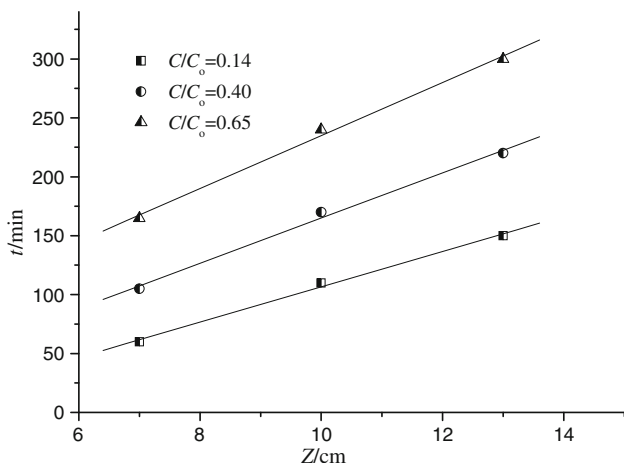


**Fig. 8** Iso-removal lines for breakthroughs of 0.14, 0.40 and 0.65, respectively, for different bed heights

*The BDST model*

The BDST model is a simple model for predicting the relationship between bed depth,  $Z$ , and service time,  $t$ , in terms of process concentrations and adsorption parameters. The BDST model is based on the assumption that the rate of adsorption is controlled by the surface reaction between adsorbate and the unused capacity of the adsorbent [44].

The values of breakthrough time obtained for various bed depth used in this study were introduced into the BDST model. A linear relationship between bed depth and service time is given by Eq. 19:

$$t = \frac{N_0 Z}{C_0 F} - \frac{1}{k_a C_0} \ln\left(\frac{C_0}{C_t} - 1\right) \tag{19}$$

A plot of bed depth,  $Z$  versus time  $t$ , should be linear, allowing the evaluation of  $N_0$  and  $k_a$ , i.e., the adsorption capacity and the rate constant, respectively.

**Table 5** Calculated constants of the BDST model for the adsorption of uranium(VI) onto CAMPS

$C/C_0$	$a$ (min cm <sup>-1</sup> )	$b$ (min)	$k_a$ (L mg <sup>-1</sup> min <sup>-1</sup> )	$N_0 \times 10^3$ (mg L <sup>-1</sup> )	$R$
0.14	15.00	43.33	$6.98 \times 10^{-4}$	7.20	0.9980
0.40	19.17	26.67	$2.53 \times 10^{-4}$	9.20	0.9993
0.65	22.50	10.00	$-1.03 \times 10^{-3}$	10.80	0.9979

A simplified form of the BDST model is:

$$t = aZ - b \tag{20}$$

where

$$a = \frac{N_0}{C_0 F} \tag{21}$$

$$b = \frac{1}{K_a C_0} \ln\left(\frac{C_0}{C_t} - 1\right) \tag{22}$$

The slope constant for a different flow rate can be directly calculated by Eq. 23:

$$a' = a \frac{F}{F'} = a \frac{Q}{Q'} \tag{23}$$

where  $a$  and  $F$  is the old slope and influent linear velocity and  $a'$  and  $F'$  is the new slope and influent linear velocity, respectively. As the column used in experiment has the same diameter, the ratio of original ( $F$ ) and the new influent linear velocity ( $F'$ ) and original flow rate ( $Q$ ) and the new flow rate ( $Q'$ ) is equal.

For other influent concentrations, the desired equation is given by a new slope, and a new intercept given by following expression:

$$a' = a \frac{C_0}{C'_0} \tag{24}$$

$$b' = b \cdot \frac{C_0}{C'_0} \cdot \frac{\ln(C'_0 - 1)}{\ln(C_0 - 1)} \tag{25}$$

where  $b'$ ,  $b$  are the new and old intercept, respectively;  $C'_0$  and  $C_0$  are the new and old influent concentration, respectively.

The plot of  $t$  versus  $Z$  at values of  $C_t/C_0$  0.14, 0.40 and 0.65 on the basis of BDST model was shown in Fig. 8. The related constants of BDST model calculated from the slopes and intercepts of the direct lines were listed in Table 5.

**Table 6** Predicted breakthrough time based on the BDST constants for a new flow rate or new influent concentration ( $Z = 10$  cm)

$C_t/C_0$	$a'$	$b'$	$T_c/\text{min}$	$t_e/\text{min}$	$E/\%$ <sup>a</sup>
$Q' = 6.0 \text{ mL min}^{-1}, C_0 = 60 \text{ mg L}^{-1}$					
0.14	20.0	43.33	157	170	8.8
0.40	25.6	26.67	229	235	2.6
0.65	30.0	10.00	290	330	12.1
$Q = 8.0 \text{ mL min}^{-1}, C_0' = 40 \text{ mg L}^{-1}$					
0.14	22.5	58.4	167	175	4.6
0.40	28.8	35.9	252	235	-7.2
0.65	33.8	13.5	325	315	-3.2

$$^a E = \frac{t_e - t_c}{t_c} \times 100\%$$

It can be seen from Table 5, as the value of  $C_t/C_0$  increased, the value of  $N_0$  increased, while the value of rate constant ( $K_a$ ) decreased. The high correlation coefficients  $R$  ( $>0.997$ ) suggested the feasibility of the BDST model for the present column system. The BDST model constants can be helpful to scale up the process for other flow rates and concentrations without further experimental operation.

The equation obtained at flow rate of  $6 \text{ mL min}^{-1}$  and influent concentration of  $40 \text{ mg L}^{-1}$  was used to predict the adsorbent performance at other flow rates or influent concentrations. The predicted time ( $t_c$ ) and experimental time ( $t_e$ ) were shown in Table 6. The results demonstrated the BDST equation can excellently predict the adsorption performance at different conditions for adsorption of uranium(VI) onto CAMPS column.

## Conclusion

Uranium(VI) adsorption onto CAMPS was investigated in batch and column modes. The kinetic, equilibrium and breakthrough curves were discussed. The kinetic process was better described by the pseudo-second-order kinetic and Elovich models while adsorption isotherm was effectively described by the Langmuir and Koble–Corrigan adsorption models. The value of  $q_m$  from the Langmuir model was  $71.59 \text{ mg g}^{-1}$ . The breakthrough curves were significantly affected by flow rate, initial uranium(VI) concentration and bed height. The column data were fitted by the Thomas, Yan and BDST models. The Yan model was best to fit the breakthrough curves at experimental conditions using nonlinear regressive analysis.

**Acknowledgments** This study was supported by the Education Department of Henan Province in China (No. 2010A610003) and Henan Science and Technology Department in China (No. 102102210103).

## References

- Donat R, Esen K, Cetisli H, Aytas S (2009) J Radioanal Nucl Chem 279:253
- Humelnicu D, Drochioiu G, Sturza MI, Cecal A, Popa K (2006) J Radioanal Nucl Chem 270:637
- Donia AM, Atia AA, Moussa MM, Sherif AM, Magied MO (2009) Hydrometallurgy 95:183
- Ganesh R, Robinson KG, Chu LL, Kucsmas D, Reed GD (1999) Water Res 33:3447
- Kryvoruchko AP, Yurlova LY, Atamanenko ID, Kornilovich BY (2004) Desalination 162:229
- Mellah A, Chegrouche S, Barkat M (2006) J Colloid Interface Sci 296:434
- Kadous A, Didi M, Villemin D (2009) J Radioanal Nucl Chem 280:157
- Sodayea H, Nisanb S, Poletikoc C, Prabhakara S, Tewaria PK (2009) Desalination 235:9
- Morsy AMA, Hussein AEM (2011) J Radioanal Nucl Chem 288:341
- Zou WH, Zhao L, Han RP (2011) J Radioanal Nucl Chem 288:239
- Zou WH, Bai HJ, Zhao L, Li K, Han RP (2011) J Radioanal Nucl Chem 288:779
- Aytas SO, Akyil S, Eral M (2004) J Radioanal Nucl Chem 260:119
- Bishay AF (2010) J Radioanal Nucl Chem 286:81
- Bagherifam S, Lakzian A, Ahmedi SJ, Rahimi MF, Halajnia A (2010) J Radioanal Nucl Chem 283:289
- Vaughan T, Seo CW, Marshall WE (2001) Bioresour Technol 78:133
- Šćiban M, Klačnja M, Škrbić B (2008) Desalination 229:170
- O'Connell DW, Birkinshaw C, O'Dwyer TF (2008) Bioresour Technol 99:6709
- Sciban M, Radetic B, Kevresan Z, Klasnja M (2007) Bioresour Technol 98:402
- Zhang H, Tang Y, Liu XN, Ke ZG, Su X, Cai DQ, Wang XQ, Liu YD, Huang Q, Yu ZL (2011) Desalination 274:97
- Misaelides P, Godelitsas A, Filippidis A, Charistos D, Anousi I (1995) Sci Total Environ 173/174:237
- Guibal E, Lorenzelli R, Vincent T, Cloirec PL (1995) Environ Technol 16:101
- Balistreri LS, Murray JW (1981) Am J Sci 281:788
- Barnett MO, Jardine PM, Brooks SC, Selim HM (2000) Soil Sci Soc Am J 64:908
- Langmuir I (1916) J Am Chem Soc 38:2221
- Freundlich HMF (1906) J Phys Chem 57:385–470
- Koble RA, Corrigan TE (1952) Ind Eng Chem 44:383
- Dubin M (1960) Chem Rev 60:235
- Hasany SM, Chaudhary MH (1996) Appl Radiat Isot 47:467
- Mahramanlioglu M, Bicer IO, Misirli T, Kilislioglu A (2007) J Radioanal Nucl Chem 273:621
- Chowdhury S, Mishra R, Saha P, Kushwaha P (2011) Desalination 265:159
- Ho YS, Ng JCY, McKay G (2000) Sep Purif Methods 29:189
- Cheung CW, Porter JF, McKay G (2000) Sep Purif Technol 19:55
- Weber WJ Jr, Morris JC (1963) Am Soc Civil Eng 89:31
- Srivastava VC, Swamy MM, Mall ID, Prasad B, Mishra IM (2006) Colloid Surf A 272:89
- Dogan M, Ozdemir Y, Alkan M (2007) Dyes Pig 75:701
- Singh KK, Rastogi R, Hasan SH (2005) J Colloid Interface Sci 290:61
- Aksu Z, Gonen F (2004) Process Biochem 39:599
- Gokhale SV, Jyoti KK, Lele SS (2009) J Hazard Mater 170:735

39. Vijayaraghavan K, Jegan J, Palanivelu K, Velan M (2004) *J Hazard Mater* 113:223
40. Thomas HC (1944) *J Am Chem Soc* 66:1664
41. Vijayaraghavan K, Prabu D (2006) *J Hazard Mater* 137:558
42. Yan G, Viraraghavan T, Chen M (2001) *Adsorpt Sci Technol* 19:25
43. Lodeiro P, Herrero R, Sastre de Vicente ME (2006) *J Hazard Mater* 137:244
44. Goel J, Kadirvelu K, Rajagopal C, Garg VK (2005) *J Hazard Mater* 125:211